Annals of Botany **122**: 1219–1229, 2018
doi: 10.1093/aob/mcy125, available online at www.academic.oup.com/aob

ANNALS OF BOTANY Founded 1887

Calcium signalling regulates the functions of the bZIP protein VIP1 in touch responses in *Arabidopsis thaliana*

Daisuke Tsugama[1,2]*, Shenkui Liu[3], Kaien Fujino[1] and Tetsuo Takano[2]

[1]Laboratory of Crop Physiology, Research Faculty of Agriculture, Hokkaido University, Kita 9 Nishi 9 Kita-ku, Sapporo-shi, Hokkaido 060-8589, Japan, [2]Asian Natural Environmental Science Center, The University of Tokyo, 1-1-1 Midori-cho, Nishitokyo-shi, Tokyo 188-0002, Japan and [3]State Key Laboratory of Subtropical Silviculture, Zhejiang A & F University, Lin'an, Hangzhou 311300, PR China
**For correspondence. E-mail: tsugama@res.agr.hokudai.ac.jp*

Received: 28 April 2018 Returned for revision: 21 May 2018 Editorial decision: 5 June 2018 Accepted: 12 June 2018
Published electronically 14 July 2018

• **Background and Aims** VIP1 is a bZIP transcription factor in *Arabidopsis thaliana*. VIP1 and its close homologues transiently accumulate in the nucleus when cells are exposed to hypo-osmotic and/or mechanical stress. Touch-induced root bending is enhanced in transgenic plants overexpressing a repression domain-fused form of VIP1 (VIP1-SRDXox), suggesting that VIP1, possibly with its close homologues, suppresses touch-induced root bending. The aim of this study was to identify regulators of these functions of VIP1 in mechanical stress responses.
• **Methods** Co-immunoprecipitation analysis using VIP1-GFP fusion protein expressed in Arabidopsis plants identified calmodulins as VIP1-GFP interactors. *In vitro* crosslink analysis was performed using a hexahistidine-tagged calmodulin and glutathione *S*-transferase-fused forms of VIP1 and its close homologues. Plants expressing GFP-fused forms of VIP1 and its close homologues (bZIP59 and bZIP29) were submerged in hypotonic solutions containing divalent cation chelators, EDTA and EGTA, and a potential calmodulin inhibitor, chlorpromazine, to examine their effects on the nuclear–cytoplasmic shuttling of those proteins. VIP1-SRDXox plants were grown on medium containing 40 mM $CaCl_2$, 40 mM $MgCl_2$ or 80 mM NaCl. MCA1 and MCA2 are mechanosensitive calcium channels, and the hypo-osmotic stress-dependent nuclear–cytoplasmic shuttling of VIP1-GFP in the *mca1 mca2* double knockout mutant background was examined.
• **Key Results** *In vitro* crosslink products were detected in the presence of $CaCl_2$, but not in its absence. EDTA, EGTA and chlorpromazine all inhibited both the nuclear import and the nuclear export of VIP1-GFP, bZIP59-GFP and bZIP29-GFP. Either 40 mM $CaCl_2$or 80 mM NaCl enhanced the VIP-SRDX-dependent root bending. The nuclear–cytoplasmic shuttling of VIP1 was observed even in the *mca1 mca2* mutant.
• **Conclusions** VIP1 and its close homologues can interact with calmodulins. Their nuclear–cytoplasmic shuttling requires neither MCA1 nor MCA2, but does require calcium signalling. Salt stress affects the VIP1-dependent regulation of root bending.

Keywords: *Arabidopsis thaliana*, bZIP transcription factor, calcium signalling, mechanical stress, nuclear-cytoplasmic shuttling, root bending, root touch responses.

INTRODUCTION

VIP1 is a bZIP transcription factors in *Arabidopsis thaliana*. Arabidopsis bZIP proteins have been classified into 11 groups (groups A–I and S, and one unnamed group) based on similarities in amino acid sequences and features, and VIP1 belongs to group I (Jakoby *et al.*, 2002). Of the 12 genes encoding the Arabidopsis group I bZIP proteins, *VIP1* and six other genes [*bZIP59* (also known as *POSF21*), *bZIP69*, *bZIP29*, *bZIP30*, *bZIP52* and *bZIP18*] are strongly expressed in seedlings, leaves, roots and flowers, while the other genes are hardly expressed in these organs. Many of the Arabidopsis group I bZIP proteins show transcriptional activation potential in a yeast one-hybrid system, can physically interact with each other (Tsugama *et al.*, 2014) and can bind DNA with the AGCTGT/G motif (Pitzschke *et al.*, 2009; Tsugama *et al.*, 2014, 2016; O'Malley *et al.*, 2016; Van Leene *et al.*, 2016).

VIP1 is thought to regulate responses to *Agrobacterium tumefaciens* and a microbe-associated molecular pattern, flg22 (Tzfira *et al.*, 2001, 2002, 2004; Lacroix *et al.*, 2005; Li *et al.*, 2005; Djamei *et al.*, 2007; Pitzschke *et al.*, 2009), although the importance of VIP1 in *Agrobacterium* responses has been partly questioned (Shi *et al.*, 2014). VIP1 also regulates leaf growth and responses to sulfur deficiency, osmotic stress and mechanical stress (Wu *et al.*, 2010; Tsugama *et al.*, 2012, 2016). bZIP29 also regulates leaf growth and mechanical stress responses (Van Leene *et al.*, 2016). bZIP30 regulates leaf growth and reproductive growth (Lozano-Sotomayor *et al.*, 2016). bZIP59 regulates salt stress-induced anthocyanin biosynthesis (Van Oosten *et al.*, 2013). In pollen grains, *bZIP18* and *bZIP52* are more strongly expressed than the other genes encoding group I bZIP proteins, and they regulate pollen fertility (Gibalová *et al.*, 2017). VSF-1, a close VIP1 homologue in tomato, is strongly expressed in vascular tissues, and regulates expression of other vascular genes (Torres-Schumann *et al.*, 1996; Ringli and Keller, 1998). RF2a and RF2b, two close VIP1 homologues in rice, also regulate vascular gene expression, and also responses to the rice tungro virus (Yin *et al.*, 1997; Petruccelli *et al.*, 2001; Dai *et al.*, 2004, 2006,

2008). RSG, a close VIP1 homologue in tobacco, regulates the biosynthesis of a phytohormone, gibberellin (Fukazawa *et al.*, 2000, 2010, 2011; Igarashi *et al.*, 2001; Ishida *et al.*, 2004, 2008; Ito *et al.*, 2010, 2014). These findings suggest that the group I bZIP proteins have pleiotropic roles.

Under steady conditions, VIP1 is phosphorylated, and interacts with 14-3-3 proteins, which retain VIP1 in the cytoplasm. When mechanical stress is imposed on Arabidopsis cells, VIP1 is dephosphorylated, and accumulates in nuclei within 10 min. VIP1 is then phosphorylated and disperses back into the cytoplasm (Tsugama *et al.*, 2012; Takeo and Ito, 2017). Putative phosphorylation sites important for this response are conserved between VIP1 and group I bZIP proteins, and at least bZIP59, bZIP69, bZIP29, bZIP30 and bZIP52 exhibit similar patterns of changes in subcellular localization (Tsugama *et al.*, 2014, 2016). A calcium-dependent protein kinase (CDPK) can phosphorylate RSG (Ishida *et al.*, 2008), and isoforms of the regulatory B″ subunit of protein phosphatase 2A (PP2A) interact with bZIP29 in Arabidopsis suspension cell cultures and seedlings (Van Leene *et al.*, 2016). CDPKs and PP2A complexes are candidate regulators of phosphorylation states of group I bZIP proteins, although it is unclear whether they are involved in mechanical stress responses. Overexpression of a repression domain-fused form of VIP1 (VIP1-SRDX) represses expression of putative VIP1 target genes and enhances touch-induced root bending, and this VIP1-SRDX-dependent root bending is suppressed by overexpression of the VIP1-GFP fusion protein, which should retain the transcriptional activation potential of VIP1. VIP1-SRDX-dependent root bending is also suppressed in the presence of either the ethylene precursor 1-aminocyclopropane-1-carboxylic acid or the synthetic auxin 2,4-dichlorophenoxyacetic acid, suggesting that VIP1 regulates ethylene and/or auxin responses. On the basis of these findings, VIP1 is thought to suppress touch-induced root bending by regulating ethylene and/or auxin responses (Tsugama *et al.*, 2016).

Here, a co-immunoprecipitation analysis identified calmodulins as VIP1-GFP interactors. Because calmodulins are calcium-binding proteins and regulate calcium signalling, interactions between VIP1 and calcium signalling were further examined.

MATERIALS AND METHODS

Plant materials

Arabidopsis thaliana ecotype Col-0 was used as the wild-type control for all experiments. Seeds of the *mca1 mca2* double mutant (Yamanaka *et al.*, 2010) were provided by Dr Hidetoshi Iida (Tokyo Gakugei University, Japan). Transgenic Arabidopsis lines overexpressing green fluorescent protein (GFP) (GFPox), VIP1-GFP (VIP1-GFPox), bZIP59-GFP (bZIP59-GFPox), bZIP29-GFP (bZIP29-GFPox) and VIP1-SRDX (VIP1-SRDXox) were prepared as previously described (Tsugama *et al.*, 2012, 2014, 2016). To express VIP1-GFP in the *mca1 mca2* background, *mca1 mca2* and VIP1-GFPox plants were crossed as the pod and pollen parents, respectively. GFP signals in the resulting F_2 and F_3 plants were briefly analysed using a BX50 epifluorescence microscope (Olympus, Tokyo, Japan), and the plants with the GFP signals were further grown until flowering. Pieces (~1 × 1 mm^2) of their cauline leaves were then ground using BioMasher II (Nippi Inc., Tokyo, Japan) in 100 µL of a homogenization buffer [250 mM NaCl, 25 mM EDTA (Wako Pure Chemical Industries, Osaka, Japan), 0.5 % (w/v) SDS (Wako) and 200 mM Tris-HCl (Wako), pH 7.5]. The resulting solutions were centrifuged at 14 000 *g* for 3 min, and the supernatants were mixed with 90 µL 2-propanol. The resulting solutions were centrifuged at 14 000 *g* for 5 min to precipitate DNA, and the supernatants were removed. The precipitated DNA was washed with 70 % (v/v) ethanol, dried and dissolved in 35 µL distilled water. Genomic PCR was performed using these DNA samples as templates and primers shown in Supplementary Data Table S1 to analyse the 35S promoter-*VIP1* region and T-DNA insertion in *MCA1* and *MCA2*. With these analyses, VIP1-GFPox plants in the *mca1 mca2* background (VIP1-GFPox/*mca*) were selected from F_3 plants, and used for further analyses.

Plant growth conditions and touch response tests

To maintain plants, seeds were surface-sterilized with 5 % (v/v) sodium hypochlorite, and sown on medium containing 0.8 % (w/v) agar (Wako), 0.5× Murashige and Skoog (MS) salts (Wako) (Murashige and Skoog, 1962), 1 % (w/v) sucrose (Wako) and 0.5 g L^{-1} MES (Dojindo Laboratories Co., Mashiki-machi, Japan), pH 5.8. Seeds were chilled at 4 °C in the darkness for 48 h, and then germinated at 22 °C. Plants were grown at 22 °C under a 16-h:8-h light–dark cycle (light intensity: 120 µmol m^{-2} s^{-1}) for 2–3 weeks on the agar media, transferred to rockwool cubes, and further grown with regular watering to collect seeds.

To evaluate touch-induced root bending, plants were grown for 10 or 15 d on the MS agar medium [1.2 % (w/v) agar, 0.5× MS salts, 1 % (w/v) sucrose, 0.5 g L^{-1}MES, pH 5.8] tilted at a 75° angle. To examine the effects of calcium deficiency, medium containing all the above components but no $CaCl_2$ was used instead. To examine effects of excessive salts, 0.5× MS agar medium supplemented with 40 mM $CaCl_2$ (Wako), 40 mM $MgCl_2$ (Wako) or 80 mM NaCl (Wako) was used instead. The plants were then photographed, and the lengths of the primary roots and the lengths of vertical projections from those roots were measured using ImageJ software (Schneider *et al.*, 2012). The vertical projection lengths were then divided by the primary root lengths to obtain vertical growth indices (VGIs) as previously described (Grabov *et al.*, 2005).

Co-immunoprecipitation

For co-immunoprecipitation to identify VIP1-GFP interactors, VIP1-GFPox plants were grown for 10 d on MS agar medium as described in the subsection above. Approximately 25 10-d-old plants were incubated in 50 mM Tris-HCl, pH 7.5, for 10 min at room temperature, and then incubated for 1 h at room temperature in 10 mL of a crosslink solution (1 mM DSP (Dojindo) and 50 mM Tris-HCl, pH 7.5). Another ~25 10-day-old plants were submerged in the crosslink solution directly, and incubated for 1 h at room temperature. The two sets of ~25 plants were then combined, and ground in 1.5 mL of a protein extraction buffer (150 mM NaCl, 1 % (v/v) Triton X-100 (Wako), 1× protease inhibitor cocktail (EDTA-free, Nacalai Tesque, Inc., Kyoto, Japan), and 50 mM Tris-HCl, pH 7.5) using a mortar and pestle. The resulting solution was centrifuged at 14000× g for 3 min, and

the supernatant was transferred to a new sample tube as a crude protein sample. To 1 mL of the crude protein sample, 150 µL of the anti-GFP mAb magnetic beads (MBL Co., Ltd, Nagoya, Japan) was added, and the resulting solution was incubated for 5 h at 4 °C with gentle shaking. The beads were then washed three times with TBS (Tris-buffered saline: 150 mM NaCl, 20 mM Tris-HCl, pH 7.5), three times with double-distilled water, and incubated at 95 °C for 5 min in 50 µL of a protein elution solution (50 mM dithiothreitol and 50 mM $NaHCO_3$). The supernatant was transferred to a new sample tube, and iodoacetamide was added to it to a 50 mM final concentration. The resulting solution was incubated for 1 h at room temperature, and diluted 20 times with double-distilled water. The resulting solution was then passed through an Amicon Ultra filter with 3-kDa cutoff (Merck Millipore, Burlington, MA, USA). The solution that remained on the filter was diluted 10 times with double-distilled water, and passed through the Amicon Ultra filter with 3-kDa cutoff once more. The solution that remained on the filter was transferred to a new sample tube, and MS-grade trypsin (Wako) was added to it to a final concentration of 3 ng μL^{-1}. The resulting solution was incubated for 3 h at 37 °C, and passed through an Ultrafree-MC filter with 0.45-µm cutoff (Merck Millipore). Peptide fragments in the filtrated solution were then analysed by LC-MS/MS using an LTQ-Orbitrap XL mass spectrometer (Thermo Fisher Scientific Inc., Waltham, MA) at the Global Facility Center at Hokkaido University. Detected peptide sequences were compared with Arabidopsis protein sequences deposited in the UniProt database (https://www.uniprot.org/) (The UniProt Consortium, 2017) to identify the proteins co-immunoprecipitated with VIP1-GFP. For a control, GFPox plants were also used for the analysis.

In vitro *protein–protein interaction analyses*

To express hexahistidine-tagged CALMODULIN1 (His-CAM1) in *Escherichia coli* and purify it, total RNA was extracted from 10-d-old wild-type seedlings using a NucleoSpin RNA Plant kit (Macheley-Nagel, Düren, Germany), and first-strand cDNA was synthesized from 500 ng total RNA using ReverTra Ace reverse transcriptase (Toyobo, Osaka, Japan) and oligo dT_{15} primer. The cDNA solution was diluted 10 times with distilled water. Using this solution as the template, the primer pair 5′-CCTGGATCCATGGCGGATCAACTCACTGACGAAC-3′ and 5′-CACCTCGAGTCACTTCATCATAATCTTGAC-3′ (*Nco*I, *Bam*HI and *Xho*I sites are underlined), and the KOD FX Neo DNA polymerase (Toyobo), the coding sequence of *CAM1* was amplified by PCR. The PCR products were digested with *Bam*HI and *Xho*I, and cloned into the *Bam*HI–*Xho*I site of pRSETB (Thermo Fisher Scientific), generating pRSET-CAM1. This construct was transformed into *E. coli* strain BL21(DE3) pLysS (Thermo Fisher Scientific). The transformed *E. coli* cells were cultured overnight at 37 °C in Luria-Bertani medium with 0.2 mM isopropyl-β-D-thiogalactopyranoside, harvested by centrifugation at 14 000 *g* for 30 s, resuspended in TBS with 1 mg mL^{-1} lysozyme (Wako), frozen in liquid nitrogen and thawed at room temperature. The freezing and thawing were repeated twice more. The resulting solution was mixed with recombinant DNase I (Takara Bio Inc., Kusatsu, Japan), incubated at room temperature until the solution became fluid, and centrifuged at 14 000 *g* for 20 min. The supernatant was transferred to a new sample tube as a crude protein sample. His-CAM1 in the crude protein sample was bound to COSMOGEL His-Accept (Nacalai Tesque) according to the manufacturer's instructions, and eluted with 200 mM imidazole. The resulting solution was diluted twice with distilled water, and passed through an Amicon Ultra filter with 3-kDa cutoff to concentrate His-CAM1. The resulting solution was used as a solution containing purified His-CAM1. Solutions containing glutathione *S*-transferase (GST)-fused full-length VIP1 (GST-VIP1) and GST-fused truncated forms of VIP1 were prepared as previously described (Tsugama *et al*., 2012, 2013*a*). Solutions containing the GST-fused C-terminal region of bZIP29, GST-fused bZIP59 and GST-fused bZIP69 were prepared as previously described (Tsugama *et al*., 2014, 2016). These GST-fused proteins were concentrated using an Amicon Ultra filter with 3-kDa cutoff. Protein concentrations in the purified protein solutions were determined using the Pierce Coomassie Plus (Bradford) assay kit (Thermo Fisher Scientific), and adjusted to 10 mg mL^{-1} with 100 mM imidazole for His-CAM1, and 30 mg mL^{-1} with 10 mM reduced glutathione in 50 mM Tris-HCl, pH 8.0, for the GST-fused proteins.

For *in vitro* crosslink assays, either EDTA or $CaCl_2$ was added to 7.5 µL of the His-CAM1 solution to a final concentration of 20 mM (for both EDTA and $CaCl_2$). The resulting solutions were mixed with 7.5 µL of the solutions containing the GST-fused proteins, and DSP was added to a final concentration of 1 mM. The resulting solutions were incubated for 1 h at room temperature, mixed with 5 µL of a non-reducing SDS sample buffer [5 % (w/v) SDS, 2.25 % (v/v) glycerol and 275 mM Tris-HCl, pH 6.8], and incubated for 5 min at 100°C. Proteins in the resulting solutions were separated by SDS-PAGE, and transferred to an Immun-Blot PVDF membrane (Bio-Rad, Hercules, CA, USA). The membrane was blocked with 3 % (w/v) skimmed milk, washed twice with TBST [TBS containing 0.1 % (v/v) Tween-20], and reacted at room temperature for 1 h with HisProbe-HRP (Thermo Fisher Scientific) diluted 2000 times with TBST. The membrane was then washed three times with TBST, and signals were detected using western BLoT Quant HRP substrate (Takara Bio) and a LumiVision Pro imager (Aisin Seiki, Nagoya, Japan). After detecting the signals, the membrane was incubated for 10 min at room temperature with gentle shaking in a stripping solution [135 mM NaCl, 0.5 % (w/v) SDS, 17 mM Tris-HCl, 25 mM EDTA, pH 8.0] to remove HisProbe-HRP, washed three times with TBST, reacted at room temperature for 1 h with a peroxidase-conjugated anti-GST antibody (Wako), and washed three times with TBST. Signals were then detected using SuperSignal West Pico chemiluminescent substrate (Thermo Fisher Scientific) and LumiVision Pro imager. Images were processed with GIMP (http://www.gimp.org/) and Inkscape (http://www.inkscape.org).

An *in vitro* pull-down assay was performed as previously described (Tsugama *et al*., 2013*b*). Briefly, GST-VIP1 was bound to Glutathione Sepharose 4B (GE Healthcare, Little Chalfont, UK) according to the manufacturer's instructions. The resulting resin was resuspended in the solution containing purified His-CAM1 and 10 mM $CaCl_2$, incubated for 1 h at room temperature with gentle shaking, washed five times with TBS, resuspended in SDS sample buffer [4 % (w/v) SDS, 10 % (w/v) sucrose, 0.01 % (w/v) bromophenol blue (Wako), 10 % (v/v) 2-mercaptoethanol and 125 mM Tris-HCl, pH 6.8], and

incubated for 5 min at 100°°C. The supernatant was subjected to SDS-PAGE followed by western blotting using HisProbe-HRP to detect His-CAM1, and then western blotting using the anti-GST antibody to detect GST-VIP1.

Yeast two-hybrid analysis

A yeast two-hybrid analysis was performed essentially as previously described (Tsugama *et al.*, 2014). Briefly, the coding sequence of *CAM1* was obtained by PCR as described in the subsection above. The PCR products were digested with *Nco*I and *Xho*I, and cloned into the *Nco*I–*Xho*I site of pGADT7-Rec (Takara Bio USA, Inc., Mountain View, CA, USA). This construct and pGBK-VIP1ΔN164 (Tsugama *et al.*, 2014) were co-transformed into the yeast strain AH109 (Takara Bio USA). Six colonies of transformed cells were streaked on the synthetic dextrose medium lacking histidine and adenine to examine protein–protein interaction-dependent activation of reporter genes.

Analyses of subcellular localization of GFP-fused proteins

To examine the effects of calcium signalling inhibitors on subcellular localization of group I bZIP proteins, GFPox, VIP1-GFPox, bZIP59-GFPox and bZIP29-GFPox plants were grown for 10 d on MS agar medium as described, incubated in a hypotonic solution (10 mM NaCl, 10 mM Tris-HCl, pH 8.0) for 0 or 10 min at room temperature, and then incubated in a 10 mM Tris-HCl (pH 8.0) solution containing 10 mM NaCl, 2 mM EDTA, 2 mM EGTA (Wako), 0.5 mM chlorpromazine hydrochloride (Wako), 1 mM $GdCl_3$ (Wako), 1 mM $LaCl_3$ (Wako) and/or 10 mM $CaCl_2$, for 10 min or 120 min (see legends to Figs 2, 3 and 5A) at room temperature. GFP signals were then detected using an epifluorescence microscope [BX51 (Olympus) equipped with a DP73 CCD camera (Olympus)]. To examine the effects of MCA1 and MCA2 on the subcellular localization of VIP1, VIP1-GFPox plants and VIP1-GFPox/*mca* plants were grown for 10 d on MS agar medium as described, incubated for 0, 10 and 120 min in 20 mM Tris-HCl, pH 8.0, and subjected to epifluorescence microscopy to detect GFP signals. Images were processed with GIMP and Inkscape.

Accession numbers

Details regarding the sequences of the genes used in this study can be obtained with the following Arabidopsis Genome Initiative accession numbers: AT1G06070 (*bZIP69*), AT1G43700 (*VIP1*), AT2G31370 (*bZIP59*), AT4G38900 (*bZIP29*), AT5G37780 (*CAM1*), AT2G17780 (*MCA2*) and AT4G35920 (*MCA1*).

RESULTS AND DISCUSSION

VIP1 interacts with calmodulin in plant cells and in vitro

Transgenic Arabidopsis plants stably expressing VIP1-GFP were reacted with the chemical cross-linker DSP when VIP1-GFP is localized to either the cytoplasm or the nucleus. VIP1-GFP in a mixture of these samples was then immunoprecipitated, and peptide fragments from co-immunoprecipitated proteins were analysed by LC-MS/MS. This analysis detected many fragments from 14-3-3 proteins, which were previously shown to interact with VIP1 (Takeo and Ito, 2017), bZIP29 (Van Leene *et al.*, 2016) and RSG (Igarashi *et al.*, 2001), validating the analysis. Fragments from calmodulin proteins, which bind calcium and can regulate functions of other proteins, were also detected (Table 1). Calmodulins are particularly interesting because calcium signalling is known to regulate root bending (Lee *et al.*, 1983*a*, *b*). This led us to further examine the interaction between VIP1 and calcium signalling.

A calmodulin, CAM1, was expressed as a hexahistidine-tagged protein (His-CAM1) in *E. coli* and purified to examine its interaction with GST-fused forms of group I bZIP proteins and their derivatives *in vitro*. A western blot of a mixture of His-CAM1, GST-VIP1, DSP and $CaCl_2$ showed one band for a hexahistidine-tagged large-sized protein, which should correspond to products of protein–protein crosslink (Fig. 1A, fourth lane in the top panel). When any of those four factors was absent from the mixture, this band was not detected (Fig. 1A, the other lanes in the top panel). These results suggest that His-CAM1 and GST-VIP1 interact *in vitro* in the presence of a sufficient amount of calcium. A corresponding band was not detected when GST was detected (Fig. 1A, bottom panels), probably because only small proportions of His-CAM1 and GST-VIP1 were crosslinked and the GST detection system was not as sensitive as the hexahistidine detection system. An *in vitro* pull-down assay failed to detect an interaction between His-CAM1 and GST-VIP1 (Fig. S1), supporting the idea that the *in vitro* interaction between His-CAM1 and GST-VIP1 is not very strong. When His-CAM1 was reacted with GST-bZIP59, GST-bZIP69 or the GST-fused C-terminal region (position 292–553), which includes the bZIP domain, of bZIP29, putative products of protein–protein crosslink were detected (Fig. 1B). The bZIP domain and its vicinity are better conserved among close VIP1 homologues than the other regions (Jakoby *et al.*, 2002; Tsugama *et al.*, 2014). The putative products of protein–protein crosslink were detected when the C-terminal region (amino acid position 165–341), which includes the bZIP domain, of VIP1 was used for the assay, but not when its N-terminal region (position 1–186) was used (Fig. 1C). Together, these results support the idea that the conserved sequences in and around the bZIP domain are responsible for the interaction between CAM1 and group I bZIP proteins. A yeast two-hybrid assay failed to detect the interaction between CAM1 and the C-terminal region of VIP1 (Fig. S2). This may be because the yeast system is not similar to either the plant system or the *in vitro* system.

Calcium signalling regulates both nuclear and cytoplasmic accumulation of VIP1

When cells are submerged in a hypotonic solution to impose mechanical stress, GFP-fused group I bZIP proteins transiently accumulate in the nuclei, and then are re-localized to the cytoplasm (Tsugama *et al.*, 2012, 2014, 2016; see Fig. 2, top row). However, the hypotonic solution-induced nuclear accumulation of the VIP1-GFP, bZIP59-GFP and bZIP29-GFP fusion proteins was not observed when a divalent cation chelator,

TABLE 1. *Proteins co-immunoprecipitated with VIP1-GFP*

Locus	Gene name	Class	Uniprot ID	Number of peptides
AT1G43700	VIP1	Group I bZIP protein	Q9MA75	16
AT2G31370	bZIP59	Group I bZIP protein	Q04088	3
AT4G09000	GRF1	14-3-3	P42643	15*
AT1G78300	GRF2	14-3-3	Q01525	14*
AT1G22300	GRF10	14-3-3	P48347	14*
AT1G35160	GRF4	14-3-3	P46077	11*
AT3G02520	GRF7	14-3-3	Q96300	10*
AT5G38480	GRF3	14-3-3	P42644	9*
AT5G16050	GRF5	14-3-3	P42645	9*
AT5G65430	GRF8	14-3-3	P48348	9*
AT5G10450	GRF6	14-3-3	P48349	8*
AT2G42590	GRF9	14-3-3	Q96299	6*
AT2G39730	RCA	RuBisCO activase	P10896	12
AT5G53620	NA	RNA polymerase II degradation factor	Q93XY1	7
AT4G20360	RABE1B	RAB GTPase homologue E1B	P17745	6
AT1G48920	NUC1/PARL1	Nucleolin	Q9FVQ1	5
AT2G21660	GRP7	Glycine-rich protein	C0Z2N6	4
AT5G37780	CAM1	Calmodulin	P0DH95	4*
AT3G56800	CAM3	Calmodulin	P0DH98	4*
AT5G21274	CAM6	Calmodulin	Q03509	4*
AT3G43810	CAM7	Calmodulin	P59220	4*
AT2G41110	CAM2	Calmodulin	F4IJ46	3*
AT1G66410	CAM4	Calmodulin	F4IEU4	3*
AT3G04120	GAPC1	Glyceraldehyde-3-phosphate dehydrogenase	P25858	4*
AT1G13440	GAPC2	Glyceraldehyde-3-phosphate dehydrogenase	Q9FX54	4*
AT3G18780	ACT2	Actin	Q96292	4*
AT1G49240	ACT8	Actin	Q96293	4*
AT3G53750	ACT3	Actin	P0CJ47	3*
AT5G09810	ACT7	Actin	P53492	3*
AT3G08580	AAC1	Mitochondrial ADP/ATP carrier	P31167	3
AT3G09440	HSP70-3	Heat shock protein 70	O65719	3
AT3G55410	NA	2-Oxoglutarate dehydrogenase, E1 component	F4IWV2	3

* These peptides are shared between proteins in the same classes.

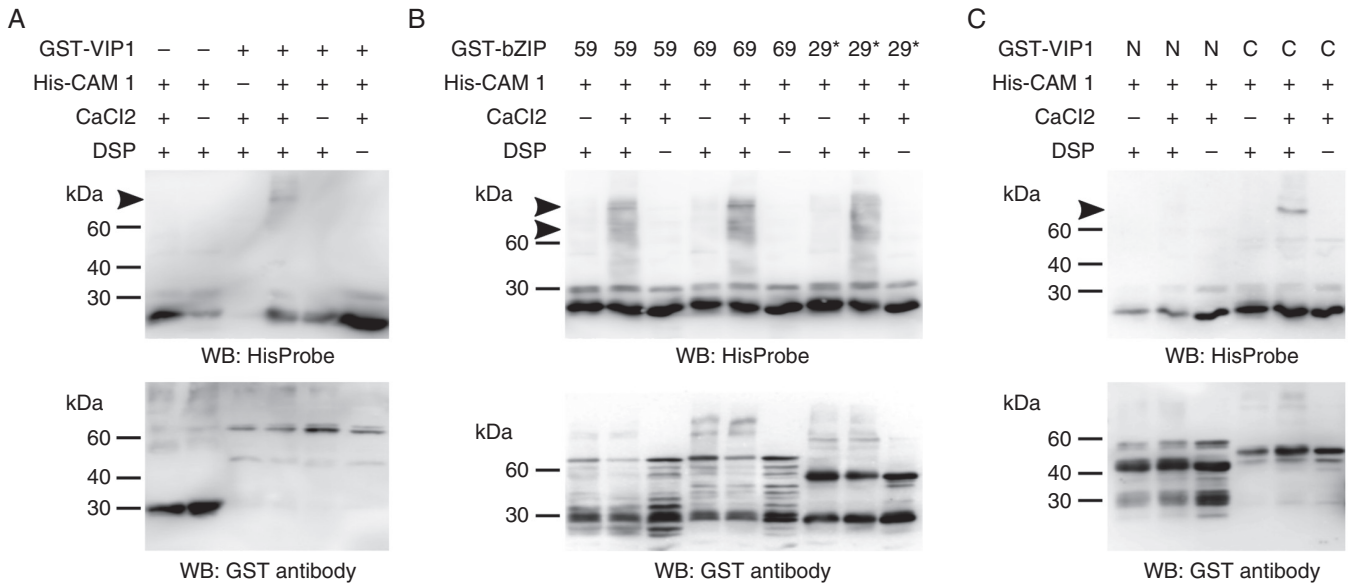

FIG. 1. Hexahistidine-tagged CAM1 (His-CAM1) interacts with GST-fused group I bZIP proteins and their derivatives *in vitro*. His-CAM1 and GST-fused proteins were expressed in *Escherichia coli*, purified, and used for *in vitro* crosslink assays. For each panel, the presence and absence of His-CAM1, GST-fused proteins, 10 mM $CaCl_2$ and 1 mM of the chemical cross-linker DSP in reaction mixtures are indicated as + and -, respectively. In reaction mixtures with $CaCl_2$, 10 mM EDTA was present. Hexahistidine was detected by western blotting with HisProbe (WB: HisProbe), and GST was detected by western blotting using an anti-GST antibody (WB: GST antibody). Arrowheads indicate putative products of protein–protein crosslink. Experiments were performed more than three times, and representative images are shown. (A) An *in vitro* crosslink assay using His-CAM1 and GST-VIP1. (B) An *in vitro* crosslink assay using His-CAM1 and GST-fused group I bZIP proteins. bZIP29* indicates the C-terminal region (amino acid position 292–553) of bZIP29. (C) An *in vitro* crosslink assay using His-CAM1 and GST-fused truncated forms of VIP1. N and C indicate the N-terminal region (amino acid position 1–186) and the C-terminal region (position 165–341) of VIP1, respectively.

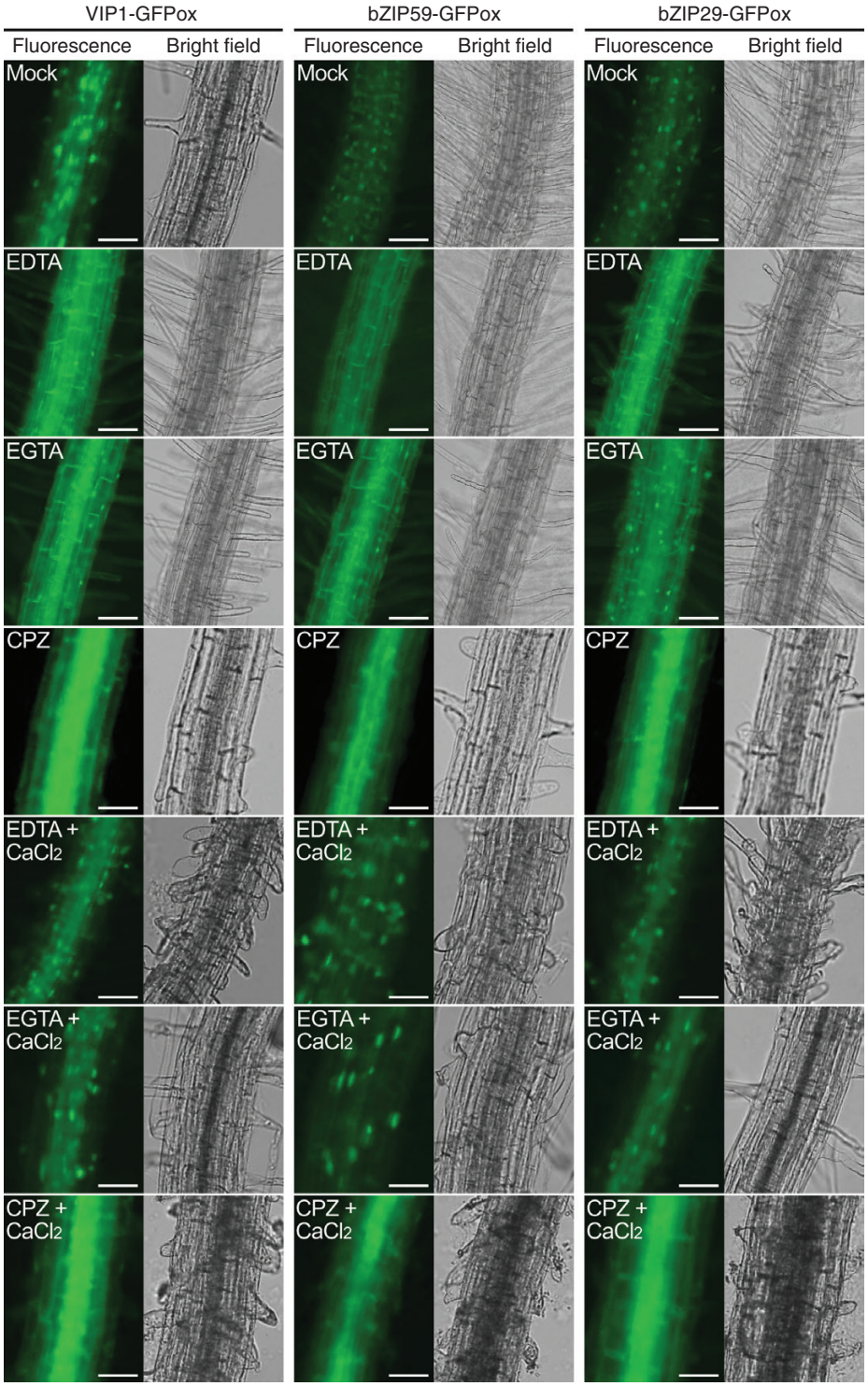

FIG. 2. Inhibitors of calcium signalling inhibit the hypotonic solution-induced nuclear accumulation of group I bZIP proteins. Ten-day-old seedlings of transgenic Arabidopsis plants overexpressing VIP1-GFP (VIP1-GFPox), bZIP59-GFP (bZIP59-GFPox) and bZIP29-GFP (bZIP29-GFPox) were incubated for 10 min in hypotonic solutions with or without 2 mM EDTA (divalent cation chelator), 2 mM EGTA, 0.5 mM chlorpromazine (CPZ) and/or 10 mM $CaCl_2$, and subjected to fluorescence microscopy to detect GFP signals in roots. For the mock treatment, 10 mM NaCl was used. For each treatment and each plant line, more than 10 individual plants were used for the analysis, and a representative image is presented. Scale bars = 50 µm.

EDTA, was present in the hypotonic solution (Fig. 2, second row). Another divalent cation chelator, EGTA, showed weaker yet similar effects (Fig. 2, third row). Chlorpromazine, which inhibits the functions of the activated (i.e. calcium-bound) form of calmodulin and decreases gravitropic responses in *Avena* coleoptiles (Biro *et al.*, 1982), also inhibited the hypotonic

solution-induced nuclear accumulation of the GFP-fused proteins (Fig. 2, fourth row). Neither EDTA nor EGTA inhibited the hypotonic solution-induced nuclear accumulation of the GFP-fused proteins when excess $CaCl_2$ was present in the hypotonic solution (Fig. 2, fifth and sixth rows). However, chlorpromazine did inhibit such nuclear localization even in the presence of excess $CaCl_2$ in the hypotonic solution (Fig. 2, seventh row). These results support the idea that calcium signalling, or calmodulin-mediated signalling in particular, is necessary for the mechanical stress-induced nuclear accumulation of group I bZIP proteins.

Interestingly, when plants were incubated in a hypotonic solution without a calcium signalling inhibitor and then transferred to a hypotonic solution with EDTA, EGTA or chlorpromazine, the GFP-fused proteins were all detected in the nuclei (Fig. 3), raising the possibility that calcium signalling is necessary for the cytoplasmic accumulation of group I bZIP proteins.

Calcium signalling may regulate phosphorylation and dephosphorylation of group I bZIP proteins. Calmodulins, isoforms of the PP2A B″ subunit, and CDPKs all have EF-hand motifs, which bind calcium, although the overall structures of these proteins should be different from each other. Although neither PP2A components nor CDPKs were detected in our co-immunoprecipitation analysis, it is still possible that not only bZIP29 and RSG but also VIP1 and other group I bZIP proteins interact with them. This idea is consistent with a previous finding that loss of function of RCN1, an isoform of the structural A subunit of PP2A, enhances root bending (Garbers *et al.*, 1996). In human cells, a calcium/calmodulin-dependent protein kinase is activated when it interacts with calmodulins, and inactivated when it interacts with PP2A complexes (Anderson *et al.*, 2004). Further studies are needed to examine the relationships between calmodulins, protein kinases, PP2A and group I bZIP proteins in plant cells.

VIP1 is involved in $CaCl_2$- and NaCl-dependent regulation of root bending

The root growth index (VGI) of the primary root is the length of the vertical projection divided by the total length, and indicates the extent of root bending (Grabov *et al.*, 2005). When grown on agar media tilted at a 45° angle, VIP1-SRDX-overexpressing (VIP1-SRDXox) plants exhibit enhanced root bending and thereby lower VGIs (Tsugama *et al.*, 2016). VIP1-SRDXox #7 plants exhibited lower VGIs than the wild type even when grown on media tilted at a 75° angle, but VIP1-SRDXox #10 and #11 plants did not. Similar results were obtained either

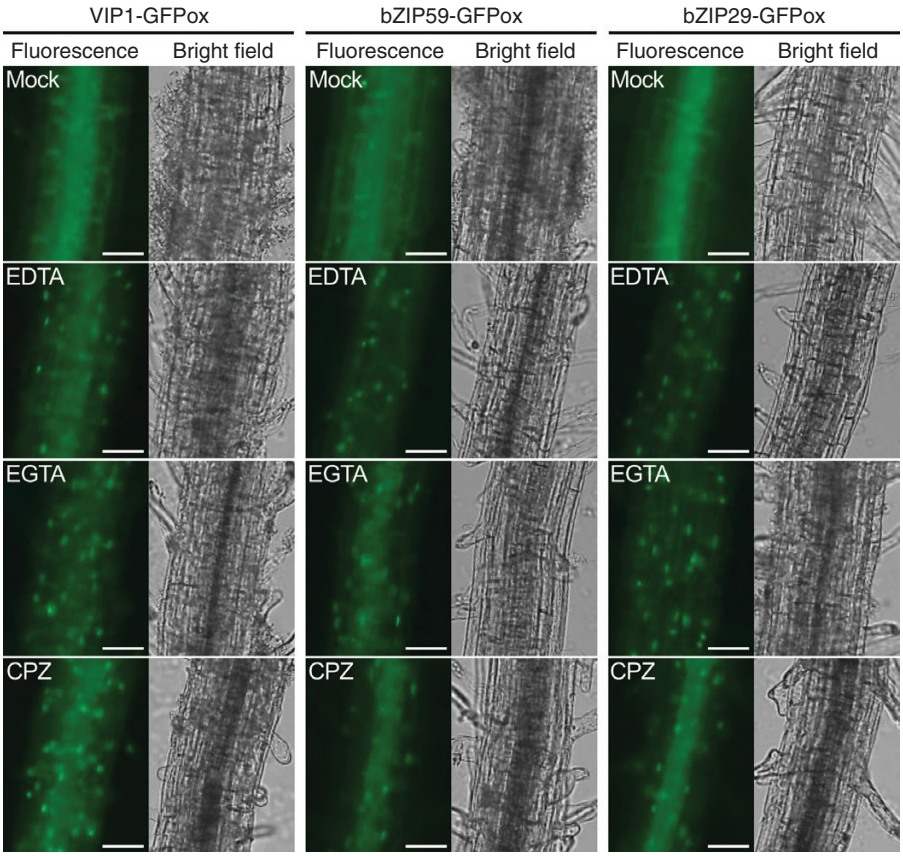

FIG. 3. Inhibitors of calcium signalling inhibit the cytoplasmic accumulation of group I bZIP proteins under hypo-osmotic conditions. Ten-day-old seedlings of transgenic Arabidopsis plants overexpressing VIP1-GFP (VIP1-GFPox), bZIP59-GFP (bZIP59-GFPox) and bZIP29-GFP (bZIP29-GFPox) were incubated for 10 min in a hypotonic solution to induce their nuclear accumulation, then incubated for 120 min in a hypotonic solution with or without 2 mM EDTA (divalent cation chelator), 2 mM EGTA or 0.5 mM chlorpromazine (CPZ), and subjected to fluorescence microscopy to detect GFP signals in roots. For the mock treatment, 10 mM NaCl was used. For each treatment and each plant line, more than 10 individual plants were used for the analysis, and a representative image is presented. Scale bars = 50 μm.

under calcium-deficient conditions or in the presence of 40 mM $MgCl_2$. However, in the presence of 40 mM $CaCl_2$, VIP1-SRDX #11 plants exhibited lower VGIs, and in the presence of 80 mM NaCl, both VIP1-SRDX #10 and #11 plants exhibited lower VGIs (Fig. 4A and B). These results raise the possibility that VIP1 is involved in $CaCl_2$- and NaCl-dependent regulation of root bending. Auxin signalling is involved in regulating NaCl-induced root bending (Galvan-Ampudia *et al.*, 2013). Lipid signalling mediated by phospholipase C and D is also thought to regulate NaCl-induced root bending (Han *et al.*, 2017). Regulators of auxin signalling and lipid signalling would be candidates for new interaction partners of VIP1 and other group I bZIP proteins. The VIP1-SRDX #7, #10 and #11 plants all exhibited decreased root growth either in the absence of $CaCl_2$ or in the presence of 40 mM $CaCl_2$. The VIP1-SRDXox #7 and #10 plants also exhibited decreased root growth in the presence of 80 mM NaCl. These results raise the possibility that the VIP1-SRDXox plants have defects in maintaining homeostasis of ion, ethylene and auxin under salt-stressed conditions.

Functions of VIP1 can be regulated independently of MCA1 and MCA2

Candidates for upstream regulators of functions of group I bZIP proteins should be proteins that change intracellular

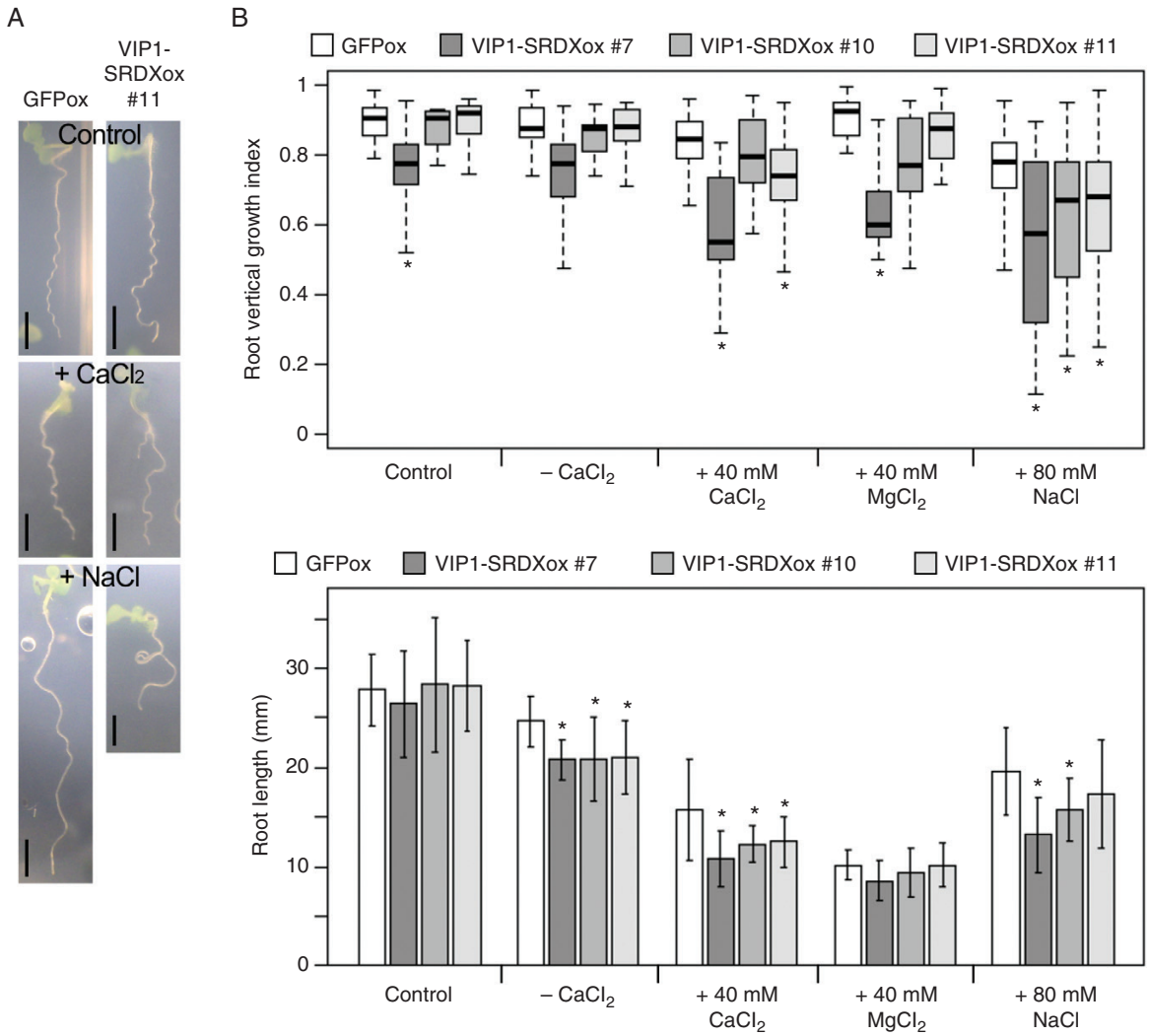

FIG. 4. Effects of salt stress on transgenic plants overexpressing GFP (GFPox) and VIP1-SRDX (VIP1-SRDXox). (A) Phenotypes of GFPox and VIP1-SRDXox #11 plants. Plants were grown for 10 d on a non-salt-stressed agar medium tilted at a 75° angle (Control) or for 15 d on an agar medium tilted at a 75° angle and containing either 40 mM $CaCl_2$ (+ $CaCl_2$) or 80 mM NaCl (+ NaCl), and photographed from the bottom of the plates through the media. One representative image is presented for each condition and each genotype. Scale bars = 0.5 mm. (B) Root vertical growth indices of GFPox and VIP1-SRDXox plants grown on agar media tilted at a 75° angle for 10 d. The control medium contained 0.5× MS salts. For – $CaCl_2$, 0.5× MS salts lacking $CaCl_2$ was used. For the other conditions, indicated concentrations of salts were added to the media. The upper and lower edges and the line in the middle of each box indicate the quartiles, and the bar corresponds to the data range (n = 38 for GFPox, Control, 14 for VIP1-SRDXox #7, Control, 36 for #10, Control, 19 for #11, Control, 17 for GFPox, – $CaCl_2$, 14 for #7, – $CaCl_2$, 19 for #10, – $CaCl_2$, 12 for #11, – $CaCl_2$, 37 for GFPox, + 40 mM $CaCl_2$, 24 for #7, + 40 mM $CaCl_2$, 34 for #10, + 40 mM $CaCl_2$, 20 for #11, + 40 mM $CaCl_2$, 16 for GFPox, + 40 mM $MgCl_2$, 14 for #7, + 40 mM $MgCl_2$, 18 for #10, + 40 mM $MgCl_2$, 8 for #11, + 40 mM $MgCl_2$, 39 for GFPox, + 80 mM NaCl, 30 for #7, + 80 mM NaCl, 21 for #10, + 80 mM NaCl, 16 for #11, + 80 mM NaCl). *P < 0.05 vs. GFPox according to the Games–Howell test (Games and Howell, 1976). (C) Primary root lengths. The data are the same as those used to calculate the vertical growth indices in the panel B, and presented as means ± s.d. *:P < 0.05 vs. GFPox according to the Games–Howell test (Games and Howell, 1976).

calcium levels in response to mechanical stress. Two such proteins are MCA1 and MCA2. These proteins are localized to the plasma membrane, and their activities are enhanced by hypo-osmotic stress and inhibited by either $GdCl_3$ or $LaCl_3$ (Nakagawa *et al.*, 2007; Yamanaka *et al.*, 2010). However, neither 1 mM $GdCl_3$ nor 1 mM $LaCl_3$ inhibited the hypotonic solution-induced nuclear accumulation of VIP1-GFP (Fig. 5A). In plants overexpressing VIP1-GFP in the *mca1 mca2* double mutant background (VIP1-GFPox/*mca*) (see Fig. S3), the pattern of the nuclear–cytoplasmic shuttling of VIP1-GFP under hypo-osmotic conditions was similar to that in VIP1-GFPox plants with the wild-type background (Fig. 5B). No differences

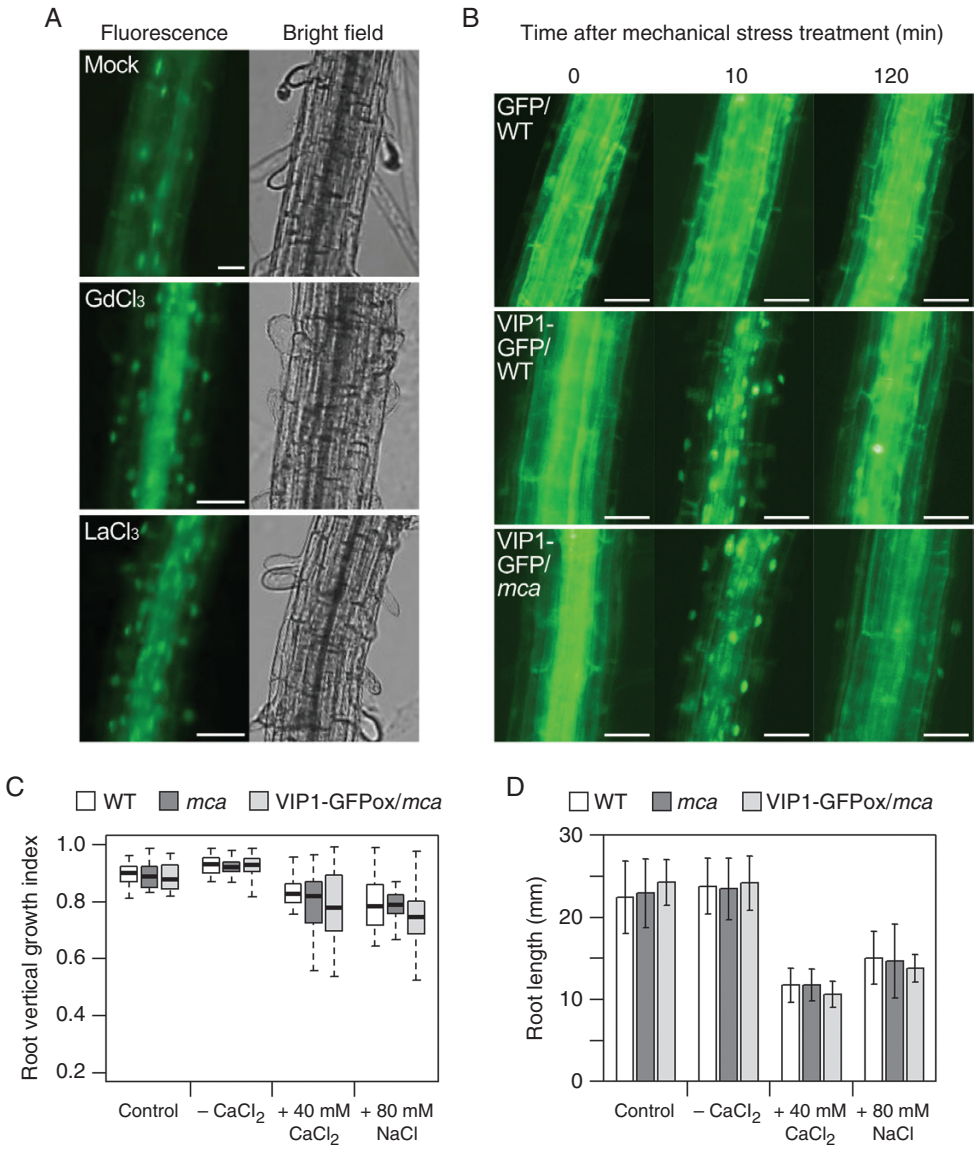

FIG. 5. Functions of VIP1 are regulated independently of MCA1 and MCA2. (A) Effects of the mechanosensitive channel inhibitors $GdCl_3$ and $LaCl_3$ on the hypotonic solution-induced nuclear accumulation of the VIP-GFP fusion protein. Transgenic plants overexpressing VIP1-GFP were incubated for 10 min in a solution without (mock) or with either 1 mM $GdCl_3$ or 1 mM $LaCl_3$, and subjected to fluorescence microscopy to detect GFP signals in roots. For each treatment, more than 10 individual plants were used for the analysis, and a representative image is presented. Scale bars = 50 µm. (B) The double null mutation *mca1 mca2* does not affect the nuclear–cytoplasmic shuttling of VIP1-GFP. The transgenic plants overexpressing GFP and VIP1-GFP in the wild-type background (GFPox/WT and VIP1-GFPox/WT, respectively) and those overexpressing VIP1-GFP in the *mca1 mca2* background (VIP1-GFPox/*mca*) were incubated in a hypotonic solution, and subjected to fluorescence microscopy to detect GFP signals in roots at the indicated time points. For each genotype, more than five individual plants were used for the analysis, and a representative image is presented for each time point. Scale bars = 50 µm. (C) Root vertical growth indices of the wild-type (WT), the *mca1 mca2* double mutant (*mca*), and VIP1-SRDXox/*mca* plants grown on agar media tilted at a 75° angle for 10 d. The control medium contained 0.5× MS salts. For – $CaCl_2$, 0.5× MS salts lacking $CaCl_2$ was used. For the other conditions, indicated concentrations of salts were added to the media. The upper and lower edges and the line in the middle of each box indicate the quartiles, and the bar corresponds to the data range (n = 15 for WT, Control, 22 for *mca*, Control, 21 for VIP1-GFPox/*mca*, Control, 32 for WT, – $CaCl_2$, 32 for *mca*, – $CaCl_2$, 46 for VIP1-GFPox/*mca*, – $CaCl_2$, 21 for WT, + 40 mM $CaCl_2$, 17 for *mca*, + 40 mM $CaCl_2$, 20 for VIP1-GFPox/*mca*, + 40 mM $CaCl_2$, 18 for WT, + 80 mM NaCl, 22 for *mca*, + 80 mM NaCl, 21 for VIP1-GFPox/*mca*, + 80 mM NaCl). No significant difference was observed (i.e. $P > 0.05$) between any samples under any condition according to the Games–Howell test (Games and Howell, 1976). (D) Primary root lengths. The data are the same as those used to calculate the vertical growth indices in the panel C, and presented as means ± s.d. No significant difference was observed (i.e. $P > 0.05$) between any samples under any condition according to the Games–Howell test (Games and Howell, 1976).

were observed between the wild type, *mca1 mca2*, and VIP1-GFPox/*mca* in either VGIs or primary root lengths under any of the conditions examined (Fig. 5C and D). These results support the idea that the functions of VIP1 are regulated independently of MCA1 and MCA2. Previously, 1 mM $GdCl_3$ almost completely inhibited mechanical stress-induced $CaCl_2$ uptake across the plasma membrane (Yamanaka *et al.*, 2010). $GdCl_3$-insensitive and/or organelle-localized mechanosensitive calcium channels may trigger the calcium signalling that regulates the functions of VIP1 and other group I bZIP proteins. Candidates for such proteins are the MSL (Msc-like) proteins MSL2 and MSL3, which are homologues of bacterial mechanosensitive ion channels and which are localized to the plastid envelope (Haswell and Meyerowitz, 2006). Two seven-transmembrane proteins, MLO4 and MLO11, and a receptor-like kinase, FERONIA, although they are not typical calcium channels, are involved in regulating both touch-induced root bending and calcium signalling (Chen *et al.*, 2009; Bidzinski *et al.*, 2014; Shih *et al.*, 2014). These proteins are also candidates for upstream regulators of the functions of group I bZIP proteins.

In conclusion, our data suggest that VIP1 and other group I bZIP proteins interact with calmodulins, and that their nuclear–cytoplasmic shuttling requires calcium signalling. VIP1-SRDX-dependent root bending is enhanced by excess NaCl or $CaCl_2$. Calcium signalling has long been known to regulate root bending, but effector proteins directly downstream of calcium signalling are largely unknown. VIP1 and other group I bZIP proteins may be such effector proteins. Further studies are needed to understand how calcium signalling and phosphorylation signalling for group I bZIP proteins interact, and which factors trigger the calcium signalling that regulates the functions of group I bZIP proteins.

SUPPLEMENTARY DATA

Supplementary data are available online at https://academic.oup.com/aob and consist of the following. Table S1: Primers used for genomic PCR. Figure S1: A pull-down assay using His-CAM1 and GST-VIP1. Figure S2: A yeast two-hybrid assay using CAM1 and the C-terminal region of VIP1. Figure S3: Genomic PCR analysis of *MCA1*, *MCA2* and the 35S promoter-*VIP1* region in VIP1-GFPox/*mca* plants.

ACKNOWLEDGMENTS

We thank Dr Hidetoshi Iida (Tokyo Gakugei University) for providing plant materials, and Ms Seiko Oka (Global Facility Center, Hokkaido University) for performing LC-MS/MS analysis and for suggestions. This work was supported by research grants from Tokyo Institute of Technology and Kato Memorial Bioscience Foundation to D.T.

LITERATURE CITED

Anderson KA, **Noeldner PK**, **Reece K**, **Wadzinski BE**, **Means AR. 2004**. Regulation and function of the calcium/calmodulin-dependent protein kinase IV/protein serine/threonine phosphatase 2A signaling complex. *The Journal of Biological Chemistry* **279**: 31708–31716.

Bidzinski P, **Noir S**, **Shahi S**, **Reinstädler A**, **Gratkowska DM**, **Panstruga R. 2014**. Physiological characterization and genetic modifiers of aberrant root thigmomorphogenesis in mutants of *Arabidopsis thaliana MILDEW LOCUS O* genes. *Plant, Cell & Environment* **37**: 2738–2753.

Biro RL, **Hale CC**, **Wiegang OF**, **Roux SJ. 1982**. Effect of chlorpromazine on gravitropism in *Avena* coleoptiles. *Annals of Botany* **50**: 737–742.

Chen Z, **Noir S**, **Kwaaitaal M *et al.* 2009**. Two seven-transmembrane domain MILDEW RESISTANCE LOCUS O proteins cofunction in Arabidopsis root thigmomorphogenesis. *Plant Cell* **21**: 1972–1991.

Dai S, **Zhang Z**, **Chen S**, **Beachy RN. 2004**. RF2b, a rice bZIP transcription activator, interacts with RF2a and is involved in symptom development of rice tungro disease. *Proceedings of the National Academy of Sciences, USA* **101**: 687–692.

Dai S, **Zhang Z**, **Bick J**, **Beachy RN. 2006**. Essential role of the Box II cis element and cognate host factors in regulating the promoter of Rice tungro bacilliform virus. *Journal of General Virology* **87**: 715–722.

Dai S, **Wei X**, **Alfonso AA *et al.* 2008**. Transgenic rice plants that overexpress transcription factors RF2a and RF2b are tolerant to rice tungro virus replication and disease. *Proceedings of the National Academy of Sciences, USA* **105**: 21012–21016.

Djamei A, **Pitzschke A**, **Nakagami H**, **Rajh I**, **Hirt H. 2007**. Trojan horse strategy in *Agrobacterium* transformation: abusing MAPK defense signaling. *Science* **318**: 453–456.

Fukazawa J, **Sakai T**, **Ishida S**, **Yamaguchi I**, **Kamiya Y**, **Takahashi Y. 2000**. Repression of shoot growth, a bZIP transcriptional activator, regulates cell elongation by controlling the level of gibberellins. *Plant Cell* **12**: 901–915.

Fukazawa J, **Nakata M**, **Ito T**, **Yamaguchi S**, **Takahashi Y. 2010**. The transcription factor RSG regulates negative feedback of *NtGA20ox1* encoding GA 20-oxidase. *The Plant Journal* **62**: 1035–1045.

Fukazawa J, **Nakata M**, **Ito T**, **Matsushita A**, **Yamaguchi S**, **Takahashi Y. 2011**. bZIP transcription factor RSG controls the feedback regulation of *NtGA20ox1* via intracellular localization and epigenetic mechanism. *Plant Signaling & Behavior* **6**: 26–28.

Galvan-Ampudia CS, **Julkowska MM**, **Darwish E *et al.* 2013**. Halotropism is a response of plant roots to avoid a saline environment. *Current Biology* **23**: 2044–2050.

Games PA, **Howell JF. 1976**. Pair wise multiple comparison procedures with unequal n's and/or variances. *Journal of Educational Statistics* **1**: 13–125.

Garbers C, **DeLong A**, **Deruére J**, **Bernasconi P**, **Söll D. 1996**. A mutation in protein phosphatase 2A regulatory subunit A affects auxin transport in Arabidopsis. *EMBO Journal* **15**: 2115–124.

Gibalová A, **Steinbachová L**, **Hafidh S *et al.* 2017**. Characterization of pollen-expressed bZIP protein interactions and the role of ATbZIP18 in the male gametophyte. *Plant Reproduction* **30**: 1–17.

Grabov A, **Ashley MK**, **Rigas S**, **Hatzopoulos P**, **Dolan L**, **Vicente-Agullo F. 2005**. Morphometric analysis of root shape. *New Phytologist* **165**: 641–651.

Han EH, **Petrella DP**, **Blakeslee JJ. 2017**. 'Bending' models of halotropism: incorporating protein phosphatase 2A, ABCB transporters, and auxin metabolism. *Journal of Experimental Botany* **68**: 3071–3089.

Haswell ES, **Meyerowitz EM. 2006**. MscS-like proteins control plastid size and shape in *Arabidopsis thaliana*. *Current Biology* **16**: 1–11.

Igarashi D, **Ishida S**, **Fukazawa J**, **Takahashi Y. 2001**. 14-3-3 proteins regulate intracellular localization of the bZIP transcriptional activator RSG. *Plant Cell* **13**: 2483–2497.

Ishida S, **Fukazawa J**, **Yuasa T**, **Takahashi Y. 2004**. Involvement of 14-3-3 signaling protein binding in the functional regulation of the transcriptional activator REPRESSION OF SHOOT GROWTH by gibberellins. *Plant Cell* **16**: 2641–2651.

Ishida S, **Yuasa T**, **Nakata M**, **Takahashi Y. 2008**. A tobacco calcium-dependent protein kinase, CDPK1, regulates the transcription factor REPRESSION OF SHOOT GROWTH in response to gibberellins. *Plant Cell* **20**: 3273–3288.

Ito T, **Nakata M**, **Fukazawa J**, **Ishida S**, **Takahashi Y. 2010**. Alteration of substrate specificity: the variable N-terminal domain of tobacco Ca^{2+}-dependent protein kinase is important for substrate recognition. *Plant Cell* **22**: 1592–1604.

Ito T, **Nakata M**, **Fukazawa J**, **Ishida S**, **Takahashi Y. 2014**. Scaffold function of Ca^{2+}-dependent protein kinase: tobacco Ca^{2+}-DEPENDENT PROTEIN KINASE1 transfers 14-3-3 to the substrate REPRESSION OF SHOOT GROWTH after phosphorylation. *Plant Physiology* **165**: 1737–1750.

Jakoby M, **Weisshaar B**, **Dröge-Laser W *et al.* bZIP Research Group**. **2002**. bZIP transcription factors in Arabidopsis. *Trends in Plant Science* **7**: 106–111.

Lacroix B, **Vaidya M**, **Tzfira T**, **Citovsky V. 2005**. The VirE3 protein of Agrobacterium mimics a host cell function required for plant genetic transformation. *The EMBO Journal* **24**: 428–437.

Lee JS, **Mulkey TJ**, **Evans ML. 1983*a***. Gravity-induced polar transport of calcium across root tips of maize. *Plant Physiology* **73**: 874–876.

Lee JS, **Mulkey TJ**, **Evans ML. 1983*b***. Reversible loss of gravitropic sensitivity in maize roots after tip application of calcium chelators. *Science* **220**: 1375–1376.

Li J, **Krichevsky A**, **Vaidya M**, **Tzfira T**, **Citovsky V. 2005**. Uncoupling of the functions of the Arabidopsis VIP1 protein in transient and stable plant genetic transformation by Agrobacterium. *Proceedings of the National Academy of Sciences, USA* **102**: 5733–5738.

Lozano-Sotomayor P, **Chávez Montes RA**, **Silvestre-Vañó M**, ***et al.* 2016**. Altered expression of the bZIP transcription factor DRINK ME affects growth and reproductive development in *Arabidopsis thaliana*. *The Plant Journal* **88**: 437–451.

Murashige T, **Skoog F. 1962**. A revised medium for rapid growth and bio assays with tobacco tissue cultures. *Physiologia Plantarum* **15**: 473–497.

Nakagawa Y, **Katagiri T**, **Shinozaki K**, ***et al.* 2007**. Arabidopsis plasma membrane protein crucial for Ca^{2+} influx and touch sensing in roots. *Proceedings of the National Academy of Sciences, USA* **104**: 3639–3644.

O'Malley RC, **Huang SC**, **Song L *et al.* 2016**. Cistrome and epicistrome features shape the regulatory DNA landscape. *Cell* **165**: 1280–1292.

Petruccelli S, **Dai S**, **Carcamo R**, **Yin Y**, **Chen S**, **Beachy RN. 2001**. Transcription factor RF2a alters expression of the rice tungro bacilliform virus promoter in transgenic tobacco plants. *Proceedings of the National Academy of Sciences, USA* **98**: 7635–7640.

Pitzschke A, **Djamei A**, **Teige M**, **Hirt H. 2009**. VIP1 response elements mediate mitogen-activated protein kinase 3-induced stress gene expression. *Proceedings of the National Academy of Sciences, USA* **106**: 18414–18419.

Ringli C, **Keller B. 1998**. Specific interaction of the tomato bZIP transcription factor VSF-1 with a non-palindromic DNA sequence that controls vascular gene expression. *Plant Molecular Biology* **37**: 977–988.

Schneider CA, **Rasband WS**, **Eliceiri KW. 2012**. NIH Image to ImageJ: 25 years of image analysis. *Nature Methods* **9**: 671–675.

Shi Y, **Lee LY**, **Gelvin SB. 2014**. Is VIP1 important for *Agrobacterium*-mediated transformation? *The Plant Journal* **79**: 848–860.

Shih HW, **Miller ND**, **Dai C**, **Spalding EP**, **Monshausen GB. 2014**. The receptor-like kinase FERONIA is required for mechanical signal transduction in Arabidopsis seedlings. *Current Biology* **24**: 1887–1892.

Takeo K, **Ito T. 2017**. Subcellular localization of VIP1 is regulated by phosphorylation and 14-3-3 proteins. *FEBS Letters* **591**: 1972–1981.

Torres-Schumann S, **Ringli C**, **Heierli D**, **Amrhein N**, **Keller B. 1996**. *In vitro* binding of the tomato bZIP transcriptional activator VSF-1 to a regulatory element that controls xylem-specific gene expression. *The Plant Journal* **9**: 283–296.

Tsugama D, **Liu S**, **Takano T. 2012**. A bZIP protein, VIP1, is a regulator of osmosensory signaling in Arabidopsis. *Plant Physiology* **159**: 144–155.

Tsugama D, **Liu S**, **Takano T. 2013*a***. Metal-binding ability of VIP1: a bZIP protein in *Arabidopsis thaliana*. *The Protein Journal* **32**: 526–532.

Tsugama D, **Liu S**, **Takano T. 2013*b***. A bZIP protein, VIP1, interacts with Arabidopsis heterotrimeric G protein β subunit, AGB1. *Plant Physiology and Biochemistry* **71**: 240–246.

Tsugama D, **Liu S**, **Takano T. 2014**. Analysis of functions of VIP1 and its close homologs in osmosensory responses of *Arabidopsis thaliana*. *PLoS One* **9**: e103930.

Tsugama D, **Liu S**, **Takano T. 2016**. The bZIP protein VIP1 is involved in touch responses in Arabidopsis roots. *Plant Physiology* **171**: 1355–1365.

Tzfira T, **Vaidya M**, **Citovsky V. 2001**. VIP1, an Arabidopsis protein that interacts with *Agrobacterium* VirE2, is involved in VirE2 nuclear import and *Agrobacterium* infectivity. *EMBO Journal* **20**: 3596–3607.

Tzfira T, **Vaidya M**, **Citovsky V. 2002**. Increasing plant susceptibility to *Agrobacterium* infection by overexpression of the Arabidopsis nuclear protein VIP1. *Proceedings of the National Academy of Sciences, USA* **99**: 10435–10440.

Tzfira T, **Vaidya M**, **Citovsky V. 2004**. Involvement of targeted proteolysis in plant genetic transformation by Agrobacterium. *Nature* **431**: 87–92.

Van Leene J, **Blomme J**, **Kulkarni SR**, ***et al.* 2016**. Functional characterization of the Arabidopsis transcription factor bZIP29 reveals its role in leaf and root development. *Journal of Experimental Botany* **67**: 5825–5840.

Van Oosten MJ, **Sharkhuu A**, **Batelli G**, **Bressan RA**, **Maggio A. 2013**. The *Arabidopsis thaliana* mutant *air1* implicates SOS3 in the regulation of anthocyanins under salt stress. *Plant Molecular Biology* **83**: 405–415.

Wu Y, **Zhao Q**, **Gao L *et al.* 2010**. Isolation and characterization of low-sulphur-tolerant mutants of Arabidopsis. *Journal of Experimental Botany* **61**: 3407–3422.

Yamanaka T, **Nakagawa Y**, **Mori K**, ***et al.* 2010**. MCA1 and MCA2 that mediate Ca^{2+} uptake have distinct and overlapping roles in Arabidopsis. *Plant Physiology* **152**: 1284–1296.

Yin Y, **Zhu Q**, **Dai S**, **Lamb C**, **Beachy RN. 1997**. RF2a, a bZIP transcriptional activator of the phloem-specific rice tungro bacilliform virus promoter, functions in vascular development. *The EMBO Journal* **16**: 5247–5259.